Path-aware Market Clearing Model for Inter-regional Electricity Market via Redundancy Elimination

Shiyuan Tao, Zhenfei Tan, Chenxing Yang, Zheng Yan, and Haihua Cheng

***Abstract*—The inter-regional electricity market is instrumental in enhancing the economic efficiency, reliability, and integration of renewable generation within interconnected power systems. As the market boundary expands, the complexity and solution difficulties of market clearing increase rapidly. The presence of hybrid alternating current (AC)/direct current (DC) interconnector networks further compounds challenges in modeling trading paths and transmission tariffs. To address these issues, this paper proposes a path-aware market-clearing (PAMC) model tailored for the inter-regional electricity market, which accommodates the hybrid AC/DC interconnector network. A variable aggregation strategy is proposed to reduce the problem scale while ensuring equivalent optimality. In addition, a novel redundancy elimination method is developed to expedite the solution of the market-clearing problem. This framework utilizes envelope approximations of residual demand curves to identify bidding blocks that will not affect the marginal price. Corresponding decision variables are then constrained to their bounds to remove redundant information. Comprehensive case studies across different power system scales validate the superiority of the proposed PAMC model in improving social welfare, and verify the effectiveness of the proposed redundancy elimination method in accelerating the solution of the market-clearing problem.**

***Index Terms*—Inter-regional electricity market, redundancy elimination, residual demand curve (RDC), transmission tariff.**

I. Introduction

INTER-REGIONAL power grids spanning vast geographical areas have been developed in various countries and regions including Europe, North America, Australia, and China. These expansive interconnected systems play a crucial role in enhancing the economic efficiency of electricity generation, ensuring the reliability of power supply, and facilitating the integration of renewable energy sources. Over the past decade, China has witnessed a sustained interest in long-distance electricity transmission. This interest arises from the increasing demand for electricity in the southern and eastern regions coupled with the growing installation of renewable generation facilities in the northern and western regions. Consequently, China has constructed an inter-provincial hybrid alternating current (AC)/direct current (DC) transmission system that encompasses over 30 ultra-high voltage transmission corridors. In 2022, the volume of electricity transmitted among provinces in China amounted to 1.77×10^{10} kWh, constituting 20.5% of the country's total electricity consumption. This figure surpasses the total electricity consumption of the European Union by more than 62.9% [1].

Electricity market reforms have consistently focused on promoting inter-regional electricity trading with the intent of optimizing electricity resource utilization across multiple regions. Since the late 1980s, the European Union has committed to establishing a unified electricity market across Europe to integrate diverse energy supplies and coordinate generation resources at the regional level [2]. The pan-European electricity market was established in different countries using a flow-based algorithm [3]. In 1998, Australia launched its National Electricity Market (NEM), one of the world's longest interconnected power systems, spanning the country's east coast [4]. Operated by the Australian Energy Market Operator (AEMO), the NEM coordinates power flow across five regional market jurisdictions based on producers and elastic customers [5]. In the United States, the electricity market is organized into various regions, each consisting of one or more states, where an independent system operator (ISO) manages each regional market. Coordinated transaction scheduling was introduced to facilitate inter-regional electricity trading, serving as an interface among different ISOs and providing a platform for external participants to engage in electricity import or export activities among regions in a market-oriented manner [6]. In 2015, China initiated a new round of electricity market reforms targeting the establishment of a nationwide unified electricity market. Provinces have played leading roles in implementing electricity mar-

Manuscript received: December 5, 2023; revised: March 20, 2024; accepted: May 22, 2024. Date of CrossCheck: May 22, 2024. Date of online publication: May 31, 2024.

This work was supported by the State Grid Corporation of China project "Research on Optimal Modeling and Fast Solution Technology of Inter-provincial Medium and Long Term Transactions Supporting Clearing with Inter-period Coupling" (No. 5100-202255381A-2-0-ZN).

S. Tao, Z. Tan (corresponding author), and Z. Yan are with the Key Laboratory of Control of Power Transmission and Conversion (Ministry of Education), and Shanghai Non-Carbon Energy Conversion and Utilization Institute, Shanghai Jiao Tong University, Shanghai 200240, China (e-mail: tsy7916@sjtu.edu.cn; zftan@outlook.com; yanz@sjtu.edu.cn).

C. Yang and H. Cheng are with China Electric Power Research Institute, Nanjing 210037, China (e-mail: yangchenxing@epri.sgcc.com.cn; chenghaihua@epri.sgcc.com.cn).

DOI: 10.35833/MPCE.2023.000962

kets, with inter-provincial markets launched to facilitate coordination among provinces [7], [8].

China's electricity market operates on a two-level system consisting of inter- and intra-provincial markets organized at the provincial level. Similar to other electricity markets worldwide, inter-provincial electricity trading in China follows a clearing process based on offers and bids submitted by participants with the aim of maximizing the total social welfare. However, some unique designs are used in China's inter-provincial markets. First, due to the hierarchical management of power grid assets, transmission tariffs are explicitly levied for each MWh of inter-provincial trading in China. Consequently, every inter-provincial transaction must specify the interconnectors it utilizes, which is a critical aspect of transmission tariff evaluation. In this paper, interconnectors are defined as trading paths. Given the extensive nature of China's inter-provincial market, which involves 27 participating provinces, a significant number of interconnectors exist that have limited capacities. Enumerating the possible trading paths and modeling path-aware transmission tariffs during the clearing process present considerable challenges. Second, the presence of numerous market entities poses computational challenges to solving the market-clearing problem. China currently boasts over 500000 market participants, a number that is expected to increase with the ongoing development of inter-provincial markets. Accordingly, accommodating this growing number of entities while ensuring efficient clearing computations presents an ongoing challenge for market operators. In addition, a market entity may simultaneously submit multiple bids, indirectly expanding the number of decision variables. For instance, a thermal power producer often divides its maximum output into multiple blocks for bidding, with each block featuring different prices, as its marginal cost increases continuously with the total output. Furthermore, the market-clearing problem must be solved across various timescales. Initial calculations are performed for annual transactions, followed by subsequent iterations for monthly and weekly transactions. This iterative clearing process considerably increases the computational burden.

In various countries and regions worldwide, regional markets display diverse development patterns. In China, each province operates its internal market independently with distinct system operators. Consequently, each provincial market is regarded as a region, whereas the inter-regional market, more specifically, the inter-provincial market, involves multiple provinces. For consistency, we employ the terms "inter-regional" and "intra-regional" to differentiate between inter-provincial and provincial markets. Concerning the modeling of the inter-regional electricity market, the European market has traditionally employed an available transfer capability (ATC)-based coupling algorithm for modeling inter-regional transmission corridors [9], enabling transition to a flow-based coupling algorithm for market clearing [10]. Studies have explored the treatment of the power of DC interconnectors as controllable variables when modeling an AC interconnector network [11]. However, few studies have been conducted on the modeling and enumeration of trading paths in hybrid AC/DC interconnector networks. In China's current market design, a sorting algorithm is utilized to clear the inter-regional market in accordance with the merit order matchmaking (MOM) rule. In previous studies, the MOM rule was formulated as an optimization problem solvable using off-the-shelf solvers in prior research [12]. However, the MOM clearing results in a social welfare loss in the presence of congestion, as demonstrated in the case study presented herein. In terms of transmission tariff allocation, multiple methods exist including postage stamp [13], MW-mile [14], and power-flow tracing [15] methods. These methods evaluate post-clearing transmission tariffs. However, in China's electricity market, the transmission tariff must be integrated into the clearing model to affect the clearing results, which is a factor not addressed in the existing literature. Some studies have proposed an inter-provincial market-clearing model that incorporates trading paths [16], [17]. However, both models simplify the hybrid AC/DC interconnector network, limiting the consideration of all trading paths.

Research on security-constrained unit commitment can provide insight into a solution algorithm for electricity market clearing. Reference [18] proposed an optimization-based approach for identifying umbrella constraints to eliminate unnecessary security constraints. References [19]-[21] analyzed the unit commitment problem and derived sufficient conditions for redundant constraints. However, the complexity of path-aware inter-regional market clearing stems primarily from the large number of decision variables rather than security constraints. In [22], an algorithm based on optimality conditions was developed to simultaneously identify redundant variables and constraints. However, this identification process requires solving the multi-integer linear programming (MILP) problem, which is inefficient and overlooks matching relationships and trading paths. Many researchers have developed methods to reduce the problem size in linear programming. Reference [23] conducted research on pre-solving for linear programming and proposed a pre-solving procedure. Reference [24] summarized five methods for identifying redundant constraints in linear programming and compared their computational efficiencies. Currently, most redundancy identification methods focus on identifying redundant constraints, with fewer studies focusing on identifying redundant variables.

In this paper, the discourse on inter-regional markets focuses on China's inter-provincial market, with issues addressed by reflecting the developmental status of this market. To align with the practical requirements of the efficient modeling and clearing of China's inter-regional electricity market, a path-aware clearing model tailored to hybrid AC/DC interconnector networks is introduced. In addition, a novel redundancy identification method is developed to expedite the solution to the market-clearing problem by eliminating redundant decision variables. This paper makes three key contributions to the literature.

1) A unified trading path model is introduced that leverages DC equivalence and transmission tariff aggregation in AC networks. This simplifies the enumeration of the trading paths within a hybrid AC/DC interconnector network. Unlike

the simplification in some existing studies, this equivalence is precise and can enumerate all trading paths in the network.

2) A path-aware market-clearing (PAMC) model is developed specifically for China's inter-regional electricity market. This model includes explicit formulations of the transmission tariffs and trading-pair matchmaking. In addition, a variable aggregation strategy is proposed to condense the market-clearing model into an equivalent form, thereby reducing the problem scale. Compared with the prevailing MOM method, this model demonstrates superior performance in enhancing social welfare, particularly in scenarios with network congestion.

3) A novel redundancy elimination method is devised to expedite the solution to the market-clearing problem. This method identifies and eliminates redundant decision variables that converge to their bounds at an optimal level through collaborative calculations across regions. Through integration of the bidding information for each region into the envelopes of the bidding curves (supply and demand), the amount of data involved in calculations is significantly reduced, making the computation of pivotal bid intervals more manageable. Unlike approximate methods for computing pivotal bids, this method calculates the interval in which pivotal bids lie (referred to as the "net export range" in this paper), ensuring that accurate clearing results are free from errors. This method enhances the computational efficiency of inter-regional electricity market clearing and presents a novel strategy for optimizing problems by eliminating redundancies.

II. PAMC Model for Inter-regional Markets

A. Trading Path Modeling on Hybrid AC/DC Interconnector Network

1) Trading Paths in Inter-regional Market

In the inter-regional electricity market, trading paths denote sequences of consecutive transmission corridors linking sending and receiving regions devoid of loops. China's inter-regional transmission network is a hybrid system consisting of both DC and AC interconnectors. Given the controllability of the power flow on DC interconnectors [25], each sending region can export power via any DC interconnector linked to its regional network and reciprocally to receiving regions. Consequently, potential trading paths exhibit combinatorial complexity relative to the number of regions and DC interconnectors.

2) Transmission Tariff Aggregation of AC Network

In contrast to DC interconnectors, where power flow can be controlled autonomously, power flow in an AC network adheres to Kirchhoff's laws. A transaction between two regions may induce power flow across multiple AC interconnectors. Consequently, the transmission tariff on a trading path involving AC interconnectors is contingent on the power flow throughout the entire AC network. Consider an AC network consisting of N nodes, with node N set as the reference node. Within the inter-regional electricity market context, the intra-regional network is disregarded, and each region is regarded as a trading node. Based on the DC power flow model, the power flow column vector $\boldsymbol{F}$ can be expressed as:

$$\boldsymbol{Y}_{ac}\boldsymbol{\theta}=\boldsymbol{P}_{inj} \tag{1}$$

$$\boldsymbol{F}=diag(\boldsymbol{y}_l)\boldsymbol{A}_{ac}^{\mathrm{T}}\boldsymbol{\theta} \tag{2}$$

where $\boldsymbol{\theta}$ is the nodal phase angle vector; $\boldsymbol{P}_{inj}$ is the nodal power injection vector; $\boldsymbol{Y}_{ac}$ is the admittance matrix of order $N-1$, excluding the reference node; $\boldsymbol{y}_l$ is the vector comprising the admittance of each branch; and $\boldsymbol{A}_{ac}$ is the node branch incident matrix with $N-1$ rows. Equation (1) is the power flow equation, and (2) evaluates the power flow vector on the AC interconnectors.

The power transfer distribution factor (PTDF) can then be derived as:

$$\boldsymbol{S}=diag(\boldsymbol{y}_l)\boldsymbol{A}_{ac}^{\mathrm{T}}\boldsymbol{Y}_{ac}^{-1}=\left[\boldsymbol{S}_1\ \boldsymbol{S}_2\ \ldots\ \boldsymbol{S}_{N-1}\right] \tag{3}$$

where $\boldsymbol{S}$ is divided into a series of column vectors $\boldsymbol{S}_u$, which estimate the power flow in the AC interconnectors caused by one unit of power transferred from node r to reference node N. For the reference node, $\boldsymbol{S}_N=\boldsymbol{0}$. This is because the power injected at the reference node does not affect the branch power flow. In the DC power flow model, the transmission of one unit of power from nodes u to v is equivalent to the transmission of power initially from nodes u to N and subsequently from nodes N to v.

Therefore, the power flow caused by the transmission from nodes u to v is evaluated as:

$$\boldsymbol{F}_{u,v}=(\boldsymbol{S}_u-\boldsymbol{S}_v)p_{u,v}\quad u,v\in\{1,2,\ldots,N\} \tag{4}$$

where $p_{u,v}$ is the trading volume between nodes u and v. Then, the transmission tariff incurred by power trading from nodes u to v on the AC network is the sum of the tariffs associated with all the relevant AC interconnectors, expressed as $\pi_{u,v,ac}$ in (5).

$$\pi_{u,v,ac}=\frac{\boldsymbol{\pi}_{ac}^{\mathrm{T}}\left|\boldsymbol{F}_{u,v}\right|}{\left|p_{u,v}\right|}=\boldsymbol{\pi}_{ac}^{\mathrm{T}}\left|\boldsymbol{S}_u-\boldsymbol{S}_v\right| \tag{5}$$

where $\boldsymbol{\pi}_{ac}$ is a column vector composed of transmission tariffs of each AC interconnector.

3) DC Equivalence of AC Network

The depth-first search (DFS) method enumerates all possible trading paths from the sending to the receiving regions by sequentially accessing adjacent nodes until the entire network is traversed [26]. Although DFS can be directly applied to a network consisting solely of DC interconnectors, wherein the power flow can be independently controlled, its direct application is not feasible for hybrid networks incorporating both DC and AC interconnectors. This limitation arises from the coupling of power flows across the AC interconnectors. However, it should be noted that the power flow distribution and aggregated transmission tariff are unequivocally determined for any trading path between the two regions within the AC network, as shown in (5). Consequently, the AC network can be substituted by a radial DC network featuring lines connected to the reference node. Each path in the original AC network can then be represented by two lines in the equivalent DC network: one extending from the sending node to the reference node and the other from the reference node to the receiving node. The transmission tariff

from the sending node to the receiving node is $\boldsymbol{\pi}_{ac}^{\mathrm{T}}\left|\boldsymbol{S}_u-\boldsymbol{S}_N+\boldsymbol{S}_N-\boldsymbol{S}_v\right|=\boldsymbol{\pi}_{ac}^{\mathrm{T}}\left|\boldsymbol{S}_u-\boldsymbol{S}_v\right|$ (considering that $\boldsymbol{S}_N=\boldsymbol{0}$), which is consistent with (5). For any two nodes in a hybrid AC/DC interconnector network, the transmission tariff can be calculated as the sum of tariffs associated with the AC and DC interconnectors.

$$\pi_{u,v,s}=\sum_{l\in T_{dc,s}}\pi_l+\boldsymbol{\pi}_{ac}^{\mathrm{T}}\left|\sum_{l\in T_{eq,s}}dir(l)\cdot\boldsymbol{S}_{u(l)}\right| \tag{6}$$

where $\pi_{u,v,s}$ is the transmission tariff from nodes u to v on path s; π_l is the transmission tariff of interconnector l; $T_{dc,s}$ is the set of DC interconnectors on path s; $T_{eq,s}$ is the set of equivalent interconnectors on path s; $dir(l)$ is the direction in which the path s passed through the interconnector l, which equals to 1 in the forward direction and −1 in the reverse direction; and $u(l)$ is the starting node number of interconnector l.

In Fig. 1(a), a six-region system is employed to illustrate the DC equivalence of the AC network. As Fig. 1(b) shows, with node 6 as the reference node, the original AC network can be substituted with a radial DC network featuring three lines connected to node 6. This equivalence allows for the transformation of the hybrid AC/DC interconnector network into a unified DC network, enabling the direct application of DFS for path enumeration.

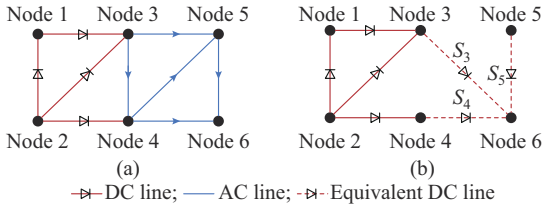

Fig. 1. Equivalence of AC network. (a) Hybrid AC/DC interconnector network. (b) Equivalent DC network.

B. PAMC Model

Following the unified trading path modeling, the PAMC model is developed. The objective (7) is to maximize the total social welfare W while minimizing transmission tariffs.

$$\max_{p_{u,v,i,j,s}} W(p_{u,v,i,j,s})=\sum_{u,v,s}\sum_{i\in G_u}\sum_{j\in C_v}(b_{v,j}-c_{u,i}-\pi_{u,v,s})p_{u,v,i,j,s} \tag{7}$$

where $p_{u,v,i,j,s}$ is the trading volume between producer i in region u and consumer j in region v; G_u is the set of producers in region u; C_v is the set of consumers in region v; $b_{v,j}$ is the bidding price of consumer j in region v; and $c_{u,i}$ is the bidding price of producer i in region u.

Constraints are given as follows.

$$\boldsymbol{F}=\sum_{u,v,s}\sum_{i\in G_u}\sum_{j\in C_v}\boldsymbol{M}_{u,v,s}p_{u,v,i,j,s} \tag{8}$$

$$P_{u,i,\min}^{g}\le\sum_{v,s}\sum_{j\in C_v}p_{u,v,i,j,s}\le P_{u,i,\max}^{g} \tag{9}$$

$$P_{v,j,\min}^{d}\le\sum_{u,s}\sum_{i\in G_u}p_{u,v,i,j,s}\le P_{v,j,\max}^{d} \tag{10}$$

$$\boldsymbol{F}_{\min}\le\boldsymbol{F}\le\boldsymbol{F}_{\max} \tag{11}$$

where $P_{u,i,\min}^{g}$ and $P_{u,i,\max}^{g}$ are the minimum and maximum limits of producer trading volumes, respectively; $P_{v,j,\min}^{d}$ and $P_{v,j,\max}^{d}$ are the minimum and maximum limits of consumer trading volumes, respectively; $\boldsymbol{F}_{\min}$ and $\boldsymbol{F}_{\max}$ are the minimum and maximum power limits of the interconnectors, respectively; and $\boldsymbol{M}_{u,v,s}$ is a column vector that represents the power flow distribution on each interconnector in the hybrid AC/DC interconnector network. According to the interconnector type, $\boldsymbol{M}_{u,v,s}$ can be divided into two parts as follows.

$$\boldsymbol{M}_{u,v,s}=\begin{bmatrix}\boldsymbol{T}_{u,v,s}\\ \boldsymbol{S}_{u,v,s}\end{bmatrix} \tag{12}$$

where $\boldsymbol{T}_{u,v,s}$ and $\boldsymbol{S}_{u,v,s}$ are the vectors corresponding to the DC and AC interconnectors, respectively.

The element in $\boldsymbol{T}_{u,v,s}$ is 1, −1, or 0, depending on the DC interconnectors in path s from nodes u to v. If the interconnector is in the positive direction, the element is 1; otherwise, it is −1. If the interconnector is not included in the path, the element is 0. $\boldsymbol{S}_{u,v,s}$ depends on the AC network or the equivalent DC network. This can be calculated from the PTDF and is derived as:

$$\boldsymbol{S}_{u,v,s}=\sum_{l\in T_{eq,s}}dir(l)\cdot\boldsymbol{S}_{u(l)} \tag{13}$$

C. Condensed Model Reformulation

Although the original PAMC model utilizes linear programming, the solution to this problem is not trivial. The PAMC determines the trading volume pairs between producers and consumers across all feasible trading paths. This leads to a significant number of decision variables, posing challenges to solving the market-clearing problem. For instance, in a system consisting of two regions, with M producers in the sending region, N consumers in the receiving region, and L trading paths connecting the two regions, the decision variable in the original PAMC model is $dim(p_{u,v,i,j,s})=MNL$. This dimension escalates rapidly with an increase in participants and trading paths, thereby intensifying the computational complexity of market clearing.

In response to the efficiency demands of calculating an inter-regional market with numerous participants and intricate interconnector networks, we develop a streamlined PAMC model. This condensed version maintains equivalence to the original model but involves fewer decision variables. In the condensed PAMC model, we reduce the dimensions of the decision variable by consolidating each consumer's trading volume across various trading paths. The original decision variables $p_{u,v,i,j,s}$ are merged along dimensions i and (v,j,s), respectively, i.e.,

$$p_{u,v,j,s}=\sum_{i\in G_u}p_{u,v,i,j,s} \tag{14}$$

$$p_{u,i}=\sum_{v,s}\sum_{j\in C_v}p_{u,v,i,j,s} \tag{15}$$

This aggregation yields two new decision variables: $p_{u,v,j,s}$ is the trading volume of consumer j in region v through trading path s originating from region u; and $p_{u,i}$ is the electricity sold by producer i in region u. Note that the output of each producer $p_{u,i}$ is an independent variable because producers no longer need to match consumers. When variable aggregation is leveraged, the condensed PAMC model can be

reformulated in three steps.

First, the objective function of the PAMC is reformulated using the aggregated decision variable:

$$\sum_{u,v,s}\sum_{i\in G_u}\sum_{j\in C_v}(b_{v,j}-c_{u,i}-\pi_{u,v,s})p_{u,v,i,j,s}-\sum_{u,v,s}\sum_{i\in G_u}\sum_{j\in C_v}(b_{v,j}-\pi_{u,v,s})p_{u,v,i,j,s}-\sum_{u,v,s}\sum_{i\in G_u}\sum_{j\in C_v}c_{u,i}p_{u,v,i,j,s}=\sum_{u,v,s}\sum_{j\in C_v}\tilde{b}_{u,v,j,s}p_{u,v,j,s}-\sum_{u}\sum_{i\in G_u}c_{u,i}p_{u,i} \tag{16}$$

$$\tilde{b}_{u,v,j,s}=b_{v,j}-\pi_{u,v,s} \tag{17}$$

This transformation can be interpreted as the conversion of consumer bidding to each sending region by incorporating transmission tariffs into different trading paths.

Second, based on the aggregated variables defined in (14) and (15), the market-clearing constraints (8)-(11) are rewritten as:

$$\boldsymbol{F}=\sum_{u,v,s}\sum_{j\in C_v}\boldsymbol{M}_{u,v,s}p_{u,v,j,s} \tag{18}$$

$$P^{g}_{u,i,\min}\le p_{u,i}\le P^{g}_{u,i,\max} \tag{19}$$

$$P^{d}_{v,j,\min}\le\sum_{u,s}p_{u,v,j,s}\le P^{d}_{v,j,\max} \tag{20}$$

$$\boldsymbol{F}_{\min}\le\boldsymbol{F}\le\boldsymbol{F}_{\max} \tag{21}$$

Third, an additional constraint is introduced to represent the power balance in each region:

$$\sum_{v,s}\sum_{j\in C_v}p_{u,v,j,s}=\sum_{i\in G_u}p_{u,i} \tag{22}$$

This constraint can be derived from (14) and (15), ensuring that the quantity of electricity sold by each region to its consumers is equivalent to the quantity of electricity generated.

Under these three steps, the condensed PAMC model is constructed by objective function (16) and constraints (18)-(22). For the aforementioned two-region instance, the decision variable dimension of the condensed model is reduced to $\dim(p_{u,v,i,j,s})=M+NL$ under the conditions given in the first paragraph of Section II-C. This reduction alleviates the complexity of formulating the model and reduces the computational burden in solving it. Note that the derivations in (14)-(22) are based on variable substitution and equation transformation, ensuring that the optimality of the condensed PAMC model remains equivalent to the original one. However, because the decision variables are aggregated, the condensed PAMC model only determines the optimal selling volume of producers and the optimal buying volume of consumers across different regions. The matching relationships between producers and consumers must be restored after the condensed PAMC model is solved. Let $p^{*}_{u,i}$ and $p^{*}_{u,v,j,s}$ denote the optimal solution of the condensed PAMC model. With $p^{*}_{u,i}$ and $p^{*}_{u,v,j,s}$, (14) and (15) become underdetermined equations of $p_{u,v,i,j,s}$. According to the matchmaking rule, trading pairs $p_{u,v,i,j,s}$ with a larger price spread (i.e., larger $b_{v,j}-c_{u,i}-\pi_{u,v,s}$), will be set to their maximum values with higher priority.

III. Accelerated Solution via Redundancy Elimination

The condensed formulation of the PAMC model successfully reduces the problem scale. However, the problem scale may be considerable in the presence of numerous participants and interconnectors. To further reduce the scale and expedite the solution to the problem, a redundancy elimination method is devised. This method leverages the market competition status of various regions.

A. Redundant Variables in PAMC Model

In a marginal-price-based market-clearing problem, the determination of the clearing results is restricted by the number of marginal units. For instance, if the bidding price falls below the marginal price, it is cleared at the minimum capacity; conversely, if the bidding price exceeds the marginal price, it is cleared at the maximum capacity. By contrast, in production offers, lower-priced offers are cleared at the maximum capacity, whereas higher-priced offers are cleared at the minimum capacity. This observation suggests a way to expedite the solution of the PAMC problem by identifying redundant variables that remain consistently bound.

Definition 1 (redundant variable): decision variables associated with bidding blocks to be cleared at minimum or maximum capacity. $p_{u,i}$ is redundant if $p^{*}_{u,i}=p^{g}_{u,i,\min}$ or $p^{*}_{u,i}=p^{g}_{u,i,\max}$. $p_{u,v,j,s}$ is redundant if $\sum_{u,s}p^{*}_{u,v,j,s}=0$ or $\sum_{u,s}p^{*}_{u,v,j,s}=p^{d}_{v,j,\max}$.

Identifying and fixing redundant variables at their lower or upper bounds in advance can significantly reduce the scale of market-clearing problems. However, preemptively identifying redundant variables before solving the market-clearing problem remains an open challenge, and no off-the-shelf method is currently available to address this issue.

B. Residual Demand Curve (RDC)-based Redundancy Identification

Determining whether a variable is redundant depends on its bidding price relative to the other bidding blocks. In the inter-regional market, identifying redundant variables involves comparing their bidding prices with the aggregated supply and demand curves of other participants. When no coupling constraints exist among the participants (i.e., no network limits exist), obtaining the supply and demand curves for the entire system is straightforward. However, with inter-regional transmission tariffs and network limits, estimating the aggregated supply and demand curves becomes feasible only for individual regions. Thus, the redundant variables must be identified separately for each region.

Consider the four-region system in Fig. 2(b). To identify redundant variables for Region A, we partition the entire system into two parts, one encompassing the studied Region A, and the other comprising the external market that includes regions B, C, and D as well as the interconnector network. As the intra-regional network is not considered in the inter-regional market, the net supply curve (NSC) represents the aggregated supply and demand information for the studied region. However, for an external system that incorporates an interconnector network, the RDC should be employed to represent the aggregated supply and demand information [27]. The NSC and RDC are defined as follows.

Definition 2 (NSC): the NSC of a region is its aggregated net generation willingness at different prices.

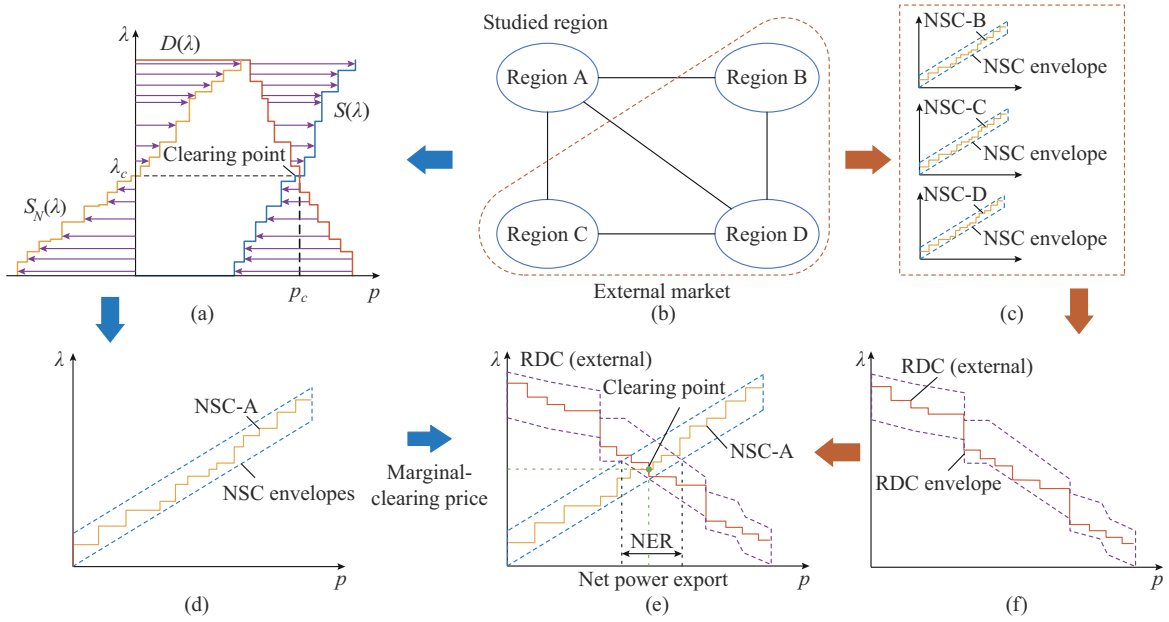

Fig. 2. Procedures for redundancy identification based on NSC and RDC. (a) Calculation of NSC. (b) Division of multi-regional system. (c) NSCs and their regions of external regions. (d) NSC and its region of studied region. (e) Calculation of NER from NSC and RDC regions. (f) Calculation of RDC region from NSC regions of external regions.

Let $S(\lambda)$ and $D(\lambda)$ denote the aggregated supply and demand curves of the region, respectively, where λ is the market price. No transmission tariffs or network limitations in this region. Therefore, the NSC of the region can be evaluated based on the difference between the supply and demand:

$$S_N(\lambda)=S(\lambda)-D(\lambda) \tag{23}$$

The calculation of the NSC is illustrated by the yellow curve in Fig. 2(a), where the blue curve is the supply curve $S(\lambda)$; the red curve is the demand curve $D(\lambda)$; and the purple arrows is the differences between supply and demand.

Definition 3 (RDC): the RDC of the external system is the aggregate electricity demand required by the external market in the studied region at different prices.

The optimization of the external system is coupled with inter-regional network constraints and transmission tariffs, and therefore, the RDC cannot be directly estimated from the difference between the aggregate supply and demand curves of the external market. Consequently, estimating the RDC mathematically requires solving the following parametric programming problem:

$$D_R(\lambda)=\underset{p_u}{\arg\max}\,(W(\boldsymbol{p})-\boldsymbol{\pi}_p^{\mathrm{T}}\boldsymbol{p}_{path}) \tag{24}$$

s.t.

$$\Omega(\boldsymbol{p},\boldsymbol{p}_{path})=0 \tag{25}$$

$$\boldsymbol{p}_{\min}\le\boldsymbol{p}\le\boldsymbol{p}_{\max} \tag{26}$$

$$\boldsymbol{F}_{\min}\le\boldsymbol{f}(\boldsymbol{p})\le\boldsymbol{F}_{\max} \tag{27}$$

$$p_u=H(\boldsymbol{p}):\lambda_u \tag{28}$$

where $\boldsymbol{p}$ is a column vector consisting of the trading volumes of all producers and consumers in the external system and is the decision variable of the problem; $\boldsymbol{\pi}_p$ is a column vector composed of transmission tariffs of each trading path; $\boldsymbol{p}_{path}$ is a column vector composed of transaction volumes of each path; $\Omega(\cdot)$ is the relationship between $\boldsymbol{p}$ and $\boldsymbol{p}_{path}$; $\boldsymbol{p}_{\min}$ and $\boldsymbol{p}_{\max}$ are the upper and lower limits of the declared power; and $\boldsymbol{f}(\cdot)$ is a function that represents the relationship between the interconnector power flow and the clearing power. The objective function is social welfare $W(\boldsymbol{p})$ minus the total tariffs on all trading paths. Constraint (25) indicates that the power exported from each region is equal to the difference between the total generation and consumption in that region. Constraint (26) restricts the upper and lower bounds of each participant's trading volume. Constraint (27) restricts the upper and lower bounds of interconnector power flow. Function $H(\boldsymbol{p})$ in (28) calculates the net export of electricity from region u to the external market, which is equal to the residual demand of the external market. The dual variable λ_u is the marginal price of the studied region, which is the parameter of this problem. The parametric solution $p_u=R(\lambda_u)$ of this problem is the RDC. For Region A, the RDC of the external system is represented by the red curve in Fig. 2(f).

If the NSC and RDC are calculated accurately, the exact market-clearing results for Region A can be obtained from the intersection of the NSC and RDC, as shown in Fig. 2(e). The marginal-clearing price and net power export of Region A are the vertical and horizontal coordinates of the intersection point, respectively. The bidding blocks in Region A with prices higher or lower than the marginal-clearing price yield redundant variables.

However, solving the parametric programming problem defined by (24)-(28) to obtain the RDC is generally challenging and often more time-consuming than directly solving the original PAMC model [28]. This complexity arises because the analytical solution to a parametric programming problem constitutes a piecewise function of the parameter, rendering the task of finding a functional solution more intricate than that of finding a single-point solution. In this paper, RDC

serves to pinpoint bidding blocks that are consistently bound at the optimum, thereby diminishing the problem scale. The objective is not necessarily to identify all redundant variables precisely; rather, identifying a subset of redundant variables is adequate to reduce the scale and expedite the solution process. To achieve this objective, envelope approximations of the NSC and RDC are employed as alternatives to efficiently identify redundancies. The fundamental concept of redundancy identification is visually elucidated in the subsequent subsection, and the mathematical models and methods are described in Section III-C and Section III-D.

The process of identifying redundant variables through envelope approximations of the NSCs and RDCs is illustrated as shown in Fig. 2. In Fig. 2(c), the NSC of each external region is enveloped by two parallel lines. Via the NSC envelopes, the RDC envelope of the entire external market can be calculated, as indicated by the purple dashed curve in Fig. 2(f). The detailed calculation process is provided in Appendix A. This envelope estimates the clearing price range of Region A at different levels of power exchange with the external system. Redundant variables are identified by comparing the RDC envelope with the NSC envelope of Region A. As Fig. 2(e) shows, the intersection of the NSC and RDC envelopes determines the potential range of energy exports of Region A in market clearing, which is termed the net export range (NER). The exact clearing point lies within the NER. Bidding blocks within the NER may become marginal, whereas those outside the NER are always cleared at the lower or upper bounds, thus becoming redundant variables. Detailed methods for calculating the NSC envelopes and the NER are introduced in the following two subsections.

C. Approximation of NSC Envelopes

To approximate the range and trend of the NSC, two parallel lines are used to form an envelope enclosing the NSC, as shown in Fig. 2(d). These envelope lines are parameterized using the slopes and intercepts. Let K denote the slope of the envelope line, which can be determined from the slope of the line connecting the left and right ends of the NSC.

$$K=\frac{S_N^{-1}(P_{\max})-S_N^{-1}(P_{\min})}{P_{\max}-P_{\min}} \tag{29}$$

where $S_N^{-1}(p)$ is the inverse function of $S_N(\lambda)$; and $P_{\min}$ and $P_{\max}$ are the minimum and maximum power export capacities of the region, respectively. Rigorously speaking, function $S_N(\lambda)$ is piecewise constant and is not invertible mathematically. Thus, we provide a detailed definition of its inverse function $S_N^{-1}(p)$ in Appendix B.

Let $B_{\min}$ and $B_{\max}$ denote the intercepts of the lower and upper envelope lines, respectively. These should be determined to ensure that the NSC is enclosed exactly by the two lines. For any point (p,λ) on the NSC, it should lie between the lower and upper envelope lines. Therefore, the intercepts must satisfy:

$$Kp+B_{\min}\le\lambda\le Kp+B_{\max} \tag{30}$$

The intercepts can then be determined by:

$$B_{\min}=\min\{S_N^{-1}(p)-Kp|P_{\min}\le p\le P_{\max}\} \tag{31}$$

$$B_{\max}=\max\{S_N^{-1}(p)-Kp|P_{\min}\le p\le P_{\max}\} \tag{32}$$

The NSC envelope can be determined using the slopes and intercepts. It depicts the range of power-exchange willingness of a region at different prices. Using an envelope to approximate the stepwise NSC reduces the representation complexity. Although the original NSC requires multiple variables to model different bidding blocks, the envelope approximation requires only four parameters (slopes and intercepts) to represent the upper and lower envelope lines. The bidding curve of each province can be approximated by a linear function, thereby simplifying the redundancy identification.

D. Calculation of NER Based on NSC Envelopes

The NER was determined by the overlapping range of the NSC and RDC envelopes in the studied region. As Fig. 2(e) shows, the right endpoint of the NER is where the lower NSC envelope intersects the upper RDC envelope, and the left endpoint is where the upper NSC envelope intersects the lower RDC envelope.

The exact clearing point, i.e., the intersection of the exact NSC and RDC, can be solved by:

$$\max_{p_u}\sum_{u\in S_R}W(p_u)-\sum_{u\in S_R}\sum_{v\in S_R}\sum_{s}\pi_{u,v,s}p_{u,v,s} \tag{33}$$

s.t.

$$W(p_u)=-\int_0^{p_u}S_{N,u}^{-1}(p)\mathrm{d}p\quad\forall u\in S_R \tag{34}$$

$$p_u=\sum_{v\in S_R}\sum_{s}p_{u,v,s}-\sum_{v\in S_R}\sum_{s}p_{v,u,s}\quad\forall u\in S_R \tag{35}$$

$$P_{u,\min}\le p_u\le P_{u,\max}\quad\forall u\in S_R \tag{36}$$

$$\boldsymbol{F}_{\min}\le\sum_{u,v,s}\boldsymbol{M}_{u,v,s}p_{u,v,s}\le\boldsymbol{F}_{\max} \tag{37}$$

where S_R is the set of all regions; $S_{N,u}^{-1}(p)$ is the inverse function of the supply curve in region u; the decision variable p_u is the net export energy of region u; $p_{u,v,s}$ is the trading volume on path s from regions u to v; and $P_{u,\min}$ and $P_{u,\max}$ are the minimum and maximum limits of the net export power of region u, respectively.

The objective is to maximize the total social welfare while minimizing the total transmission tariffs. Constraint (34) calculates the social welfare of each region, obtained as the integral of the NSC of each region. It should be noted that although the social welfare of each region is defined in the form of an integral, it is consistent with (7). The social welfare in (7) has a discrete form. Constraint (35) ensures power balance in each region, and constraints (36) and (37) represent the limits of net export power and interconnector transmission capacity, respectively.

When the exact NSC functions $S_{N,u}^{-1}(p)$ in (34) are substituted into their envelopes, the aforementioned problem can be used to calculate the upper and lower bounds of the NER. To calculate the correct endpoint of the NER, $S_{N,u}^{-1}(p)$ should be replaced by:

$$S_{N,u}^{-1}(p)=\begin{cases}K_u p+B_{u,\max} & u\in S_{ER}\\ K_u p+B_{u,\min} & u\notin S_{ER}\end{cases} \tag{38}$$

where S_{ER} is the set of external regions; K_u is the slope of the envelope line in region u; and $B_{u,\max}$ and $B_{u,\min}$ are the intercepts of the upper and lower envelope lines in region u, respectively.

The left endpoint of the NER can be calculated by replacing $S_{N,u}^{-1}(p)$ with:

$$S_{N,u}^{-1}(p)=\begin{cases} K_u p+B_{u,\min} & u\in S_{ER} \\ K_u p+B_{u,\max} & u\notin S_{ER} \end{cases} \tag{39}$$

This can be interpreted as a relationship between supply and demand. If the net supply of each external region is minimized, i.e., $B_u=B_{u,\max}$, and the net supply of the studied region is maximized, i.e., $B_u=B_{u,\min}$, the net export of the studied region will reach its maximum, and vice versa for the minimum net export.

In summary, the NER of each region is evaluated using the following three steps.

Step 1: choose a region as the studied region and solve the problem in (33)-(37) under the conditions given in (38) to obtain the maximum net exports.

Step 2: resolve the problem under the conditions outlined in (39) to obtain the minimum net exports. The NER of this region is then determined based on the maximum and minimum net exports.

Step 3: switch to another region as the studied region, and repeat *Steps 1* and *2* until the NERs of all regions are determined.

To obtain the NERs for all N regions, the problems described by (33)-(37) must be solved $2N$ times, where N is the number of regions. As the NSC envelopes in (38) and (39) are linear functions, the social welfare function in (34) is quadratic. This is referred to as quadratic programming. The number of decision variables is equal to the number of regions, which is generally small compared with the model forming each bidding block as a decision variable. Therefore, the computation of NERs is inexpensive. In addition, the NERs of different regions can be calculated in parallel, further reducing the required computation time.

E. Solution Process with Redundancy Elimination

The proposed redundancy elimination method must be executed collaboratively by inter-regional market organizers and various regions. The process of solving the PAMC with redundancy identification is as follows.

1) Each region computes the linear envelope approximation of its NSC based on (29), (31), and (32) and then reports the envelope lines to the inter-regional market operator.

2) Utilizing the NSC envelopes from different regions, the inter-regional market operator calculates the NER for each region and transmits it to the corresponding region. The computation of NERs for different regions is independent and can therefore be executed concurrently.

3) With the NER information, each region identifies redundant variables and fixes them to their corresponding upper or lower bounds. The bidding details for the non-redundant variables are relayed to the inter-regional market operator.

4) The inter-regional market operator solves the condensed PAMC model by considering only the effective variables of different regions to obtain the final clearing result.

This process can be implemented based on the development status of the inter-provincial market in China. First, the existing inter-provincial trading platform in China can support multi-round information exchanges between regional system operators and inter-regional systems. Second, despite adding an additional round of information exchange, the total amount of data exchange is smaller than that in the original single-round solution process. This is because regional system operators must only submit a small portion of bids, rather than submit bids from all parties in the region.

IV. Case Studies

We have tested the effectiveness of trading path modeling and the condensed PAMC model, and verified the effectiveness and computational efficiency of the proposed redundancy elimination method for solving the inter-regional electricity market. Simulations have been conducted using MATLAB 2022b on a laptop equipped with an Intel Core i7-10750H 2.6 GHz CPU and 24 GB RAM. Optimizations have been implemented using the Yalmip toolbox and translated into a format compatible with Gurobi v.9.5.2 to solve the optimization problems.

A. Results of Condensed PAMC Model

1) Test System

The four-region test system shown in Fig. 3 was employed to illustrate the solution for the condensed PAMC model. Each intra-regional network was simulated using the IEEE 24-bus system [29]. The generation capacity and electricity demand of the different regions were multiplied by the factors listed in Table I. In addition, each producer was assumed to submit five bidding blocks. Figure 4 shows the aggregated supply and demand curves for the four regions.

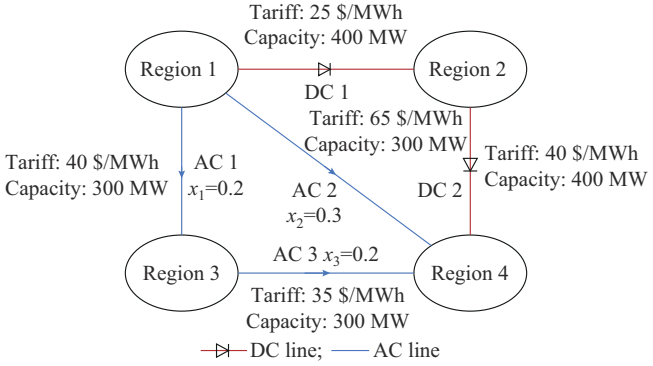

Fig. 3. Four-region test system and system parameters.

TABLE I
Capacity Multipliers for Each Region

Region	Generation multiplier	Demand multiplier
1	1.2	0.3
2	1.1	0.4
3	2.0	1.6
4	2.2	2.0

2) Trading Path Result

We enumerate the trading paths following the procedure outlined in Section II-B. Table II presents the outcomes in-

cluding the inter-regional trading paths and aggregated transmission tariffs. This case involved 24 trading paths. For paths consisting only of DC interconnectors, the aggregated transmission tariff was determined to be the sum of the tariffs of the DC interconnectors engaged. By contrast, for paths incorporating AC interconnectors, the aggregated transmission tariff of the AC network was calculated as the weighted sum of the tariffs of the AC interconnectors based on their PTDFs.

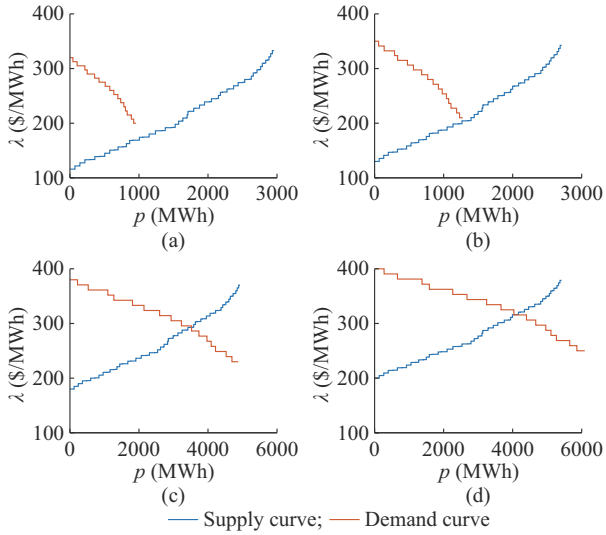

Fig. 4. Supply and demand curves of each region. (a) Region 1. (b) Region 2. (c) Region 3. (d) Region 4.

TABLE II
ENUMERATION OF ALL TRADING PATHS

Path	From region	To region	Interconnector on path	Transmission tariff ($/MWh)
1.2.1	1	2	DC1	25.00
1.2.2	1	2	AC net, DC2	109.29
1.3.1	1	3	AC net	57.14
1.3.2	1	3	DC1, DC2, AC net	120.00
1.4.1	1	4	AC net	69.29
1.4.2	1	4	DC1, DC2	65.00
2.3.1	2	3	DC1, AC net	82.14
2.3.2	2	3	DC2, AC net	95.00
2.4.1	2	4	DC2	40.00
2.4.2	2	4	DC1, AC net	94.29
3.4.1	3	4	AC net	55.00
3.4.2	3	4	AC net, DC1, DC2	122.14

With Path 1.3.2 used as an example, it is the path from Regions 1 to 3. The interconnector order was DC1, DC2, and AC net from Regions 4 to 3. The transmission tariff in the DC network was 65 $/MWh in total. In the AC network, the power flow was distributed to each AC interconnector. According to the impedance, we could calculate the PTDFs of AC1-AC3 as 0.2857, –0.2857, and –0.7143, respectively, where the minus sign means that the direction of power flow was opposite that marked in Fig. 3. The transmission tariff in the AC network could then be calculated as the weighted sum of the tariffs of each interconnector with weight coefficients as the absolute value of the PTDF, which was 55 $/MWh. In total, the transmission tariff of Path 1.3.2 was 120 $/MWh, as shown in Table II.

3) Market-clearing Result

Table III lists the inter-regional trading volumes and power flows of different interconnectors. In this case, interconnectors DC2 and AC1 reached their maximum transmission capacities. Generation and consumption data for each region are presented in Table IV. The total transmission tariff amounted to $\$9.6349 \times 10^4$, whereas the total social welfare stood at $\$1.1644 \times 10^6$.

TABLE III
TRADING PAIR RESULTS OF CONDENSED PAMC MODEL

Selling region	Purchasing region	Path	Volume (MWh)	Interconnector power flow (MWh)				
				DC1	DC2	AC1	AC2	AC3
1	3	1.3.1	489.01	0	0	349.29	139.72	–139.72
1	4	1.4.1	351.66	0	0	150.71	200.94	150.71
1	4	1.4.2	161.63	161.63	161.63	0	0	0
2	4	2.4.1	838.37	0	838.37	0	0	0
Total				161.63	1000.00	500.00	340.66	10.99

TABLE IV
GENERATION AND CONSUMPTION DATA OF EACH REGION

Region	Generation (MWh)	Generation cost (k$)	Consumption (MWh)	Consumption cost (k$)
1	1806.5	299.4	804.2	224.9
2	1878.8	350.7	1040.4	317.0
3	3247.3	739.4	3736.3	1250.9
4	3572.0	874.8	4923.7	1732.3
Total	10504.6	2264.3	10504.6	3525.1

The MOM method, currently utilized in China's inter-regional electricity market, was also used for comparison. In this clearing method, buyers and sellers are matched in descending order of spread. The trading results are outlined in Table V.

TABLE V
TRADING PAIR RESULTS OF MOM METHOD

Selling region	Purchasing region	Path	Volume (MWh)	Interconnector power flow (MWh)				
				DC1	DC2	AC1	AC2	AC3
1	2	1.2.1	66.72	66.72	0	0	0	0
1	3	1.3.1	428.94	0	0	306.38	122.55	–122.55
1	4	1.4.1	147.83	0	0	63.36	84.48	63.36
1	4	1.4.2	428.71	428.71	428.71	0	0	0
2	4	2.4.1	571.29	0	571.29	0	0	0
Total				495.43	1000.00	369.74	207.03	–59.19

The MOM method yielded a total social welfare of $\$1.1611 \times 10^6$, which was lower than that achieved by the condensed PAMC model. A comparison of the results presented in Tables III and V reveals that under the MOM method, Region 1 sold more electricity to Region 4 via Path 1.4.2 rather than Path 1.4.1 due to the higher spread. However, Path 1.4.2 shared the same interconnector DC2 with Path

2.4.1, which resulted in congestion in DC2. Consequently, Region 2 sold less electricity, resulting in a welfare loss. Thus, the MOM method may lead to social welfare losses in the presence of network congestion. By contrast, the proposed PAMC model maximized the total social welfare, outperforming the MOM method.

B. Correctness of Redundancy Elimination

The test system described in Section IV-A was used in this paper. Figure 5 shows the NSCs in each region and their envelopes. When the optimization problem in (33)-(37) was solved, the NER of each region could be obtained as shown in Fig. 5. Bidding blocks falling within the NER were considered active variables, whereas those outside the NER were considered redundant. The blocks positioned to the left and right of the NER were cleared at the maximum and minimum values, respectively. Consequently, redundant bidding blocks could be eliminated before a clear model was established.

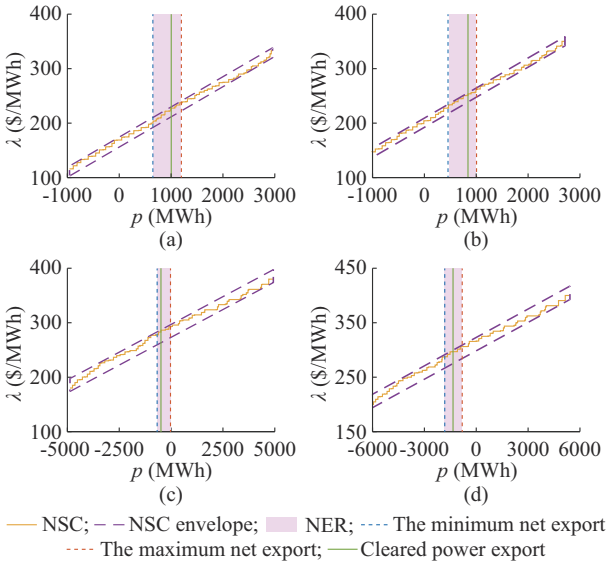

Fig. 5. NERs in each region and their envelopes. (a) Region 1. (b) Region 2. (c) Region 3. (d) Region 4.

Tabel VI lists the NERs and redundancy elimination rates for the different regions. With each region containing 77 bidding blocks, the proposed redundancy elimination method removed over 79.22% of the bidding blocks. The exact NER values of each region obtained by solving the original clearing model and falling within the NER are presented.

Notably, the clearing result of the condensed PAML model, following the elimination of redundant variables, remained consistent with that of the original model, with social welfare recorded at $\$1.1644 \times 10^6$. This substantiated the accuracy of the proposed redundancy elimination method.

C. Computational Efficiency

1) Test System

In addition to the four-region system shown in Fig. 3, 10- and 22-region systems were used to evaluate the computational efficiency of the proposed redundancy elimination method, as shown in Fig. 6.

TABLE VI
NERS AND REDUNDANCY ELIMINATION RATES FOR DIFFERENT REGIONS

Region	Cleared power export (MWh)	NER (MWh)	Price range ($/MWh)	Total bidding blocks	Eliminated bidding blocks	Elimination rate (%)
1	1002.30	[642.32, 1201.95]	[200.00, 237.50]	77	61	79.22
2	838.37	[461.00, 1000.00]	[227.59, 262.14]	77	63	81.82
3	–489.00	[–700.00, 0.00]	[277.75, 293.82]	77	71	92.21
4	–1351.66	[–1875.00, –774.96]	[287.27, 306.25]	77	67	87.01

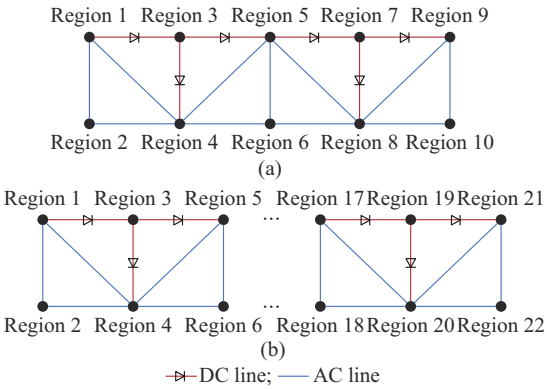

Fig. 6. Topology of 10- and 22-region systems. (a) 10-region system. (b) 22-region system.

These systems contained both AC and DC interconnectors. The IEEE 24-bus system and 500-bus synthetic systems (SG 500) [30] were used as intraregional networks to form test systems of different scales.

2) Efficiency Comparison

For each test system, the condensed PAMC model was solved using two methods: ① a direct solution without redundancy elimination, and ② an accelerated solution with redundancy elimination. The translation time of Yalmip was excluded from the solution time, and only the solution time of Gurobi was compared. The number of decision variables and computation time of the two methods were compared. The computation time of the accelerated solution method consisted of two parts: redundancy identification and market clearing. Note that redundancy identification for different regions can be executed in parallel. Thus, the computation time of this process depends on the longest time required for redundancy identification for different regions.

Table VII presents the test results. The redundancy identification process could eliminate 74.38%-86.47% of bidding blocks. The identification time depended primarily on the scale of the inter-regional system and remained largely unaffected by the scale of the intraregional system. This occurred because the number of variables involved in the identification process was dictated solely by the number of regions involved. As shown in the table, the identification phase constitutes only a minor fraction of the overall solution time, with this proportion diminishing for larger-scale intra-regional sys-

tems. In the case of systems utilizing IEEE 24-bus system, redundancy identification consists of 15.05%-41.18% of the total solution time. By contrast, for systems employing SG 500, this percentage decreases to less than 1.54%. Through the implementation of redundancy elimination, the efficiency of inter-regional market-clearing solutions is augmented by a factor of 10 to 31. In particular, in scenarios featuring large-scale intraregional systems, the acceleration of market-clearing solutions becomes notably pronounced. These findings substantiate the superior efficacy of the proposed redundancy elimination method in expediting the resolution of inter-regional market-clearing challenges involving a significant number of market participants.

For practical purposes, we supplemented another case based on the actual inter-provincial transmission network in China, which includes 25 provinces. As we do not have authentic bidding data for each region, the bidding data still use the data of the previous cases. The results are listed in the final row of Table VII. The test results showed that the redundancy identification process eliminated over 92% of the redundant variables, which was more than in previous synthetic systems. We analyzed the clearing results and found that, in this case, some regions were unable to trade any electricity because of the capacity limit of the interconnectors. Consequently, the redundancy identification process identified this and eliminated all variables in these regions.

TABLE VII
COMPUTATIONAL PERFORMANCE COMPARISON

Test system	Direct solution		Accelerated solution with redundancy elimination					
	Number of variables	Total time (s)	Variable elimination (%)	Identification time (s)	Clearing time (s)	Total time (s)	Proportion of identification time (%)	Acceleration rate
4 × IEEE 24-bus	1160	0.0180	86.47	0.0007	0.0010	0.0017	41.18	10.59
4 × SG 500	20200	1.0222	85.67	0.0005	0.0319	0.0324	1.54	31.55
10 × IEEE 24-bus	2900	0.5155	83.97	0.0068	0.0299	0.0367	18.53	14.05
10 × SG 500	50500	14.6904	80.71	0.0062	0.6325	0.6387	0.97	23.00
22 × IEEE 24-bus	6380	4.1439	79.12	0.0539	0.3042	0.3581	15.05	11.57
22 × SG 500	111100	101.1091	74.38	0.0588	4.9615	5.0203	1.17	20.14
Actual 25 regions	71510	10.9426	92.41	0.2401	0.1923	0.4324	55.53	25.31

V. CONCLUSION

To facilitate an efficient solution for inter-regional electricity market clearing, the PAMC model was proposed in this paper to accommodate hybrid AC/DC interconnector networks. This paper introduced a unified trading path model grounded in DC equivalence and the aggregation of transmission tariffs in AC networks, which streamlined the enumeration of the trading paths within a hybrid AC/DC interconnector network. The model was further enhanced with an explicit formulation of transmission tariffs and trading-pair matchmaking. A variable aggregation strategy was also devised to condense the market-clearing model into an equivalent and more manageable form, thereby reducing the problem scale. A novel redundancy elimination method leveraging the RDC was developed to expedite the solution to the market-clearing problem. Through this method, decision variables bound at the optimum could be identified and preemptively removed, thus diminishing the problem scale and enhancing the solution efficiency. Case studies conducted across diverse scales demonstrated that the proposed PAMC model outperformed the prevailing MOM method in augmenting social welfare. These findings underscored the efficacy of the proposed redundancy elimination method in accelerating inter-regional market clearing.

APPENDIX A

Rigorously speaking, function $S_N(\lambda)$ is not invertible mathematically, as it is constant in each interval. The inverse function $S_N^{-1}(p)$ in (29) should be specially defined according to its physical meaning. The definition is as follows.

First, we consider that $S_N(\lambda)$ has n intervals. The first interval is $(0, \lambda_1)$, and the second is (λ_1, λ_2), until the last is $(\lambda_{n-1}, \lambda_n)$. In each interval, the value of $S_N(\lambda)$ is p_1, p_2, ..., p_n. Then, $S_N(\lambda)$ can be expressed as:

$$S_N(\lambda)=p_i \quad \lambda \in (\lambda_{i-1}, \lambda_i), i=1,2,...,n \tag{A1}$$

We define $\lambda_0=0$, and define $S_N(\lambda)$ in open intervals because when $\lambda=\lambda_i$, $S_N(\lambda)$ can be any value between p_i and p_{i+1}.

The physical meaning of function $S_N^{-1}(p)$ is the marginal price for a given supply p. According to the expression of $S_N(\lambda)$, when p is between p_i and p_{i+1}, $S_N^{-1}(p)=\lambda_i$. Then, the function $S_N^{-1}(p)$ can be expressed as:

$$S_N^{-1}(p)=\lambda_i \quad \lambda \in (p_i, p_{i+1}), i=1,2,...,n-1 \tag{A2}$$

Similarly, $S_N^{-1}(p)$ is also defined in open intervals. If $p=p_i$, $S_N^{-1}(p)$ can be any value between λ_{i-1} and λ_i. Note that $S_N^{-1}(p)$ only has $n-1$ rather than n intervals of $S_N(\lambda)$.

APPENDIX B

The process of determining the envelope of RDC from the envelopes of NSCs is as follows.

The RDC is determined by a parametric programming problem expressed as:

$$\max_{p_u} \sum_{u \in S_{ER}} W(p_u) - \sum_{u \in S_R} \sum_{v \in S_R} \sum_{s} \pi_{u,v,s} p_{u,v,s} \tag{B1}$$

s.t.

$$W(p_u)=-\int_0^{p_u} S_{N,u}^{-1}(p)\mathrm{d}p \quad \forall u \in S_{ER} \tag{B2}$$

$$p_u=\sum_{v\in S_R}\sum_s p_{u,v,s}-\sum_{v\in S_R}\sum_s p_{v,u,s} \quad \forall u \in S_R \tag{B3}$$

$$P_{u,\min}\le p_u \le P_{u,\max} \quad \forall u \in S_R \tag{B4}$$

$$\boldsymbol{F}_{\min}\le \sum_{u,v,s}\boldsymbol{M}_{u,v,s}p_{u,v,s}\le \boldsymbol{F}_{\max} \tag{B5}$$

$$p_r=-\sum_{u\in S_{ER}} p_u : \lambda_r \tag{B6}$$

where S_{ER} is the set of external regions. In (B2), the social welfare of each region is calculated by the integral of the NSC. The relationship between the trading energy of each transaction and net export energy is expressed in (B3). Constraint (B4) limits the range of the net export energy according to the range of the NSC. Constraint (B5) is the interconnector power flow constraint, and p_r in (B6) is the residual demand, which is equal to the negative sum of the net exports of all regions. The dual variable of (B6), λ_r, is the marginal price of the studied region, which is the parameter of this problem.

As the parameter is a dual problem, directly solving the RDC is complicated and time-consuming. Therefore, in this paper, we proposed a method for estimating the range of the RDC according to the envelope of the NSC.

The NSC envelope can be expressed as:

$$Kp+B_{\min}\le\lambda\le Kp+B_{\max} \tag{B7}$$

where λ in the NSC is the marginal price of an external region. Assuming that the marginal prices of all external regions reach the upper bound (i.e. $Kp+B_{\max}$), the overall marginal price for the studied region will also reach a maximum. Accordingly, the upper bound of the RDC can be obtained by allowing all the NSCs to reach their upper bounds. In particular, the implementation method replaces the NSC function in (B2) with its upper envelope.

$$W(p_u)=-\frac{1}{2}Kp_u^2+B_{\max}p_u \quad \forall u \in S_{ER} \tag{B8}$$

As the envelope is a linear function, social welfare will be quadratic after integration, as in (B8), which is easier to solve than the original piecewise function. The lower bound of the RDC can be similarly obtained by allowing all NSCs to reach their lower bounds.

REFERENCES

[1] China Electricity Council. (2023, Jan.). Analysis and prediction report of national power supply and demand situation 2023. [Online]. Available: https://www.cec.org.cn/detail/index.html?3-317477

[2] European Union. (2015, Feb.). Energy Union factsheet. [Online]. Available: https://ec.europa.eu/commission/presscorner/detail/en/MEMO_15_4485

[3] Joint Allocation Office. (2023, Feb.). Core FB MC. [Online]. Available: https://www.jao.eu/core-fb-mc

[4] J. Bryant, P. Sokolowski, and L. Meegahapola, "Impact of FCAS market rules on Australia's national electricity market dynamic stability," in *Proceedings of 2019 IEEE International Conference on Industrial Technology*, Melbourne, Australia, Feb. 2019, pp. 637-642.

[5] Australian Energy Market Operator. (2023, Jun.). Energy markets and systems. [Online]. Available: https://www.aemo.com.au/-/media/files/electricity/nem/national-electricity-market-fact-sheet.pdf

[6] M. Ndrio, S. Bose, L. Tong *et al.*, "Coordinated transaction scheduling in multi-area electricity markets: equilibrium and learning," *IEEE Transactions on Power Systems*, vol. 38, no. 2, pp. 996-1008, Mar. 2023.

[7] M. Wang, Z. Tan, Z. Ma *et al*., "Inter-provincial electricity spot market model for China," in *Proceedings of 2020 IEEE/IAS Industrial and Commercial Power System Asia (I&CPS Asia)*, Weihai, China, Sept. 2020, pp. 110-115.

[8] IEA. (2023, Apr.). Building a unified national power market system in China. [Online]. Available: https://www.iea.org/reports/building-a-unified-national-power-market-system-in-china

[9] J. Louyrette and M. Trotignon, "European market couplings: description, modelling and perspectives," in *Proceedings of 2009 IEEE Bucharest PowerTech*, Bucharest, Romania, Jun. 2009, pp. 1-6.

[10] D. Waniek, C. Rehtanz, and E. Handschin, "Flow-based evaluation of congestions in the electric power transmission system," in *Proceedings of 2010 7th International Conference on the European Energy Market*, Madrid, Spain, Jun. 2010, pp. 1-6.

[11] Z. Tan, H. Zhong, J. Wang *et al*., "Enforcing intra-regional constraints in tie-line scheduling: a projection-based framework," *IEEE Transactions on Power Systems*, vol. 34, no. 6, pp. 4751-4761, Nov. 2019.

[12] Z. Ma, Z. Wang, J. Xiao *et al*., "A matchmaking based day-ahead market design in China," in *Proceedings of 2016 IEEE Innovative Smart Grid Technologies – Asia*, Melbourne, Australia, Nov.-Dec. 2016, pp. 132-137.

[13] H. H. Happ, "Cost of wheeling methodologies," *IEEE Transactions on Power Systems*, vol. 9, no. 1, pp. 147-156, Feb. 1994.

[14] J. Pan, Y. Teklu, S. Rahman *et al*., "Review of usage-based transmission cost allocation methods under open access," *IEEE Transactions on Power Systems*, vol. 15, no. 4, pp. 1218-1224, Nov. 2000.

[15] J. Bialek, "Tracing the flow of electricity," *IEE Proceedings*: *Generation, Transmission and Distribution*, vol. 143, no. 4, pp. 313-320, Jul. 1996.

[16] D. Zeng, Z. Yang, S. Feng *et al*., "Inter-provincial power exchange optimization modeling considering ATC constrains of hybrid AC/DC power system," *Power System Technology*, vol. 44, no. 10, pp. 3893-3899, Oct. 2020.

[17] H. Cheng, C. Yang, S. Liu *et al*., "Optimization clearing and system development of inter-provincial medium and long term trade considering ATC base on path combination," *Power System Technology*, vol. 46, no. 12, pp. 4762-4774, Dec. 2022.

[18] A. J. Ardakani and F. Bouffard, "Identification of umbrella constraints in DC-based security-constrained optimal power flow," *IEEE Transactions on Power Systems*, vol. 28, no. 4, pp. 3924-3934, Nov. 2013.

[19] Q. Zhai, X. Guan, J. Cheng *et al*., "Fast identification of inactive security constraints in SCUC problems," *IEEE Transactions on Power Systems*, vol. 25, no. 4, pp. 1946-1954, Nov. 2010.

[20] Z. Tan, Z. Yan, H. Zhong *et al*., "Non-iterative solution for coordinated optimal dispatch via equivalent projection – part I: theory," *IEEE Transactions on Power Systems*, vol. 39, no. 1, pp. 890-898, Jan. 2024.

[21] B. Hua, Z. Bie, C. Liu *et al*., "Eliminating redundant line flow constraints in composite system reliability evaluation," *IEEE Transactions on Power Systems*, vol. 28, no. 3, pp. 3490-3498, Aug. 2013.

[22] Z. Tan, H. Zhong, Q. Xia *et al*., "Non-iterative multi-area coordinated dispatch via condensed system representation," *IEEE Transactions on Power Systems*, vol. 36, no. 2, pp. 1594-1604, Mar. 2021.

[23] E. D. Andersen and K. D. Andersen, "Presolving in linear programming," *Mathematical Programming*, vol. 71, pp. 221-245, Dec. 1995.

[24] S. Paulraj and P. Sumathi. (2010, Dec.). A comparative study of redundant constraints identification methods in linear programming problems. [Online]. Available: https://onlinelibrary.wiley.com/doi/10.1155/2010/723402

[25] A. Lotfjou, M. Shahidehpour, Y. Fu *et al*., "Security-constrained unit commitment with AC/DC transmission systems," *IEEE Transactions on Power Systems*, vol. 25, no. 1, pp. 531-542, Feb. 2010.

[26] V. Palanisamy and S. Vijayanathan, "A novel agent based depth first search algorithm," in *Proceedings of 2020 IEEE 5th International Conference on Computing Communication and Automation (ICCCA)*, Greater Noida, India, Oct. 2020, pp. 443-448.

[27] T. G. Cabana, E. C. Baptista, E. M. Soler *et al*., "Optimization-based models for estimating residual demand curves for a price-maker company," *IEEE Transactions on Power Systems*, vol. 38, no. 4, pp. 3097-3106, Jul. 2023.

[28] G. Katta, "Computational complexity of parametric linear programming," *Mathematical Programming*, vol. 19, pp. 213-219, Dec. 1980.

[29] Texas A&M University Engineering. (2023, Dec.). IEEE 24-bus sys-

tem. [Online]. Available: https://electricgrids. engr. tamu. edu/electric-grid-test-cases/ieee-24-bus-system
[30] Texas A&M University Engineering. (2023, Dec.). South Carolina 500-bus system: ACTIVSg500. [Online]. Available: https://electricgrids. engr.tamu.edu/electric-grid-test-cases/activsg500

Shiyuan Tao received the B.E. degree in electrical engineering from Shanghai Jiao Tong University, Shanghai, China, in 2021. He is currently pursuing the M.E. degree in electrical engineering in Shanghai Jiao Tong University. His research interests include electricity market and optimization of power system dispatching.

Zhenfei Tan received the B.E. and Ph.D. degrees in electrical engineering from Tsinghua University, Beijing, China, in 2017 and 2022, respectively. He is currently an Assistant Professor with Shanghai Jiao Tong University, Shanghai, China. His research interests include electricity market, distributed energy resource aggregation, and coordinated optimization of hierarchical power networks.

Chenxing Yang received the Ph. D. degree in electrical engineering from Southeast University, Nanjing, China, in 2017. She is currently a Senior Engineer in China Electric Power Research Institute, Nanjing, China. Her research interests include electricity market, power grid optimal scheduling, and smart grid.

Zheng Yan received the B. S. degree from Shanghai Jiao Tong University, Shanghai, China, in 1984, and the M. S. and Ph. D. degrees from Tsinghua University, Beijing, China, in 1987 and 1991, respectively, all in electrical engineering. He is currently a Professor of Electrical Engineering with Shanghai Jiao Tong University. His current research interests include application of optimization theory to power systems, power market, and dynamic security assessment.

Haihua Cheng received the M.S. degree in electrical engineering from Wuhan University, Wuhan, China, in 2002. She is currently a Professor-level Senior Engineer in China Electric Power Research Institute, Nanjing, China. Her research interests include electricity market and power grid optimal scheduling.